

## Sample Size Dependence of Crack-tip Microstructure and Stress Evolutions in Single Crystal Nickel

Wen-Ping Wu<sup>1,2</sup>, Zong-Zhuan Yao<sup>3</sup>

**Abstract:** The internal microstructure evolution and atomic stress distribution around the crack tip of a pre-cracked single crystal nickel with unequal sample sizes are studied by molecular dynamics (MD) simulation. The simulated results indicate that the crack propagation dynamics and stress distributions around the crack tip are strongly dependent on the microstructure evolution caused by the change of sample size. Unequal sample sizes induce various atomic configurations around the crack tip during the crack propagation. When atomic configuration is invariable around the crack tip, the crack grows rapidly along the crack path, the stress concentration occurs at the crack tip of growing crack and the stress is monotonic along the crack path. Once the occurrence of microstructure evolution (void nucleation, deformation twinning) around the crack tip, the crack grows slowly and the stress value is variable along the crack path due to the peak stress is accompanied by the appearance of the void and deformation twinning ahead of the crack tip. The pre-cracked single crystal nickel under mode I loading condition shows the different crack propagation dynamics and stress distribution, which are closely related to the sample size induces void nucleation and deformation twinning mechanisms around the crack tip.

**Keywords:** Single crystal nickel, void nucleation, deformation twinning, sample size, MD simulation

### 1 Introduction

Fracture is a complex process which spans many disciplines in the physical sciences and engineering. The emergence of fracture on a macroscopic scale is a consequence of crack propagation across several length scales from atomistic to

---

<sup>1</sup> Department of Engineering Mechanics, School of Civil Engineering and Architecture, Wuhan University, Wuhan 430072, China.

<sup>2</sup> Corresponding author. Email: wpwu@whu.edu.cn

<sup>3</sup> Department of Mechanical Engineering, University of Wuppertal, Wuppertal 42097, Germany.

continuum scales. The crack progression can lead to failures in components if not detected and monitored. The driving force of crack propagation at the atomic scale is the stress field due to the loading applied to the sample. In strength theory, material failure is determined by stresses and strains. The failure analysis is directly related to the stress or strain concentration around the crack tip, because a material fails when the stress concentration exceeds the failure strength of materials. A good understanding of the failure mechanisms of materials is the key to microstructure design and property controls. With the advent of scalable parallel computers, molecular dynamics (MD) has become a very useful tool for studying the failure mechanisms of materials by investigating the microstructure evolution and mechanical properties of materials from an atomistic standpoint [Cheung and Yip(1994); Nishimura and Miyazaki (2001); Yamakov, Saether, Phillips, and Glaessgen (2006); Zhou, Zimmerman, Reedy, and Moody (2008)]. MD simulations of fracture events have produced observations that resemble characteristics at the macroscopic scales by the analysis of stress field around the crack tip. For example, [Buehler, Gao, and Huang (2004)] studied rapid mode I brittle crack propagation and showed there is a good agreement between atomistic simulation results and continuum theory predictions for the stress and strain fields around the propagating crack tip. [Matsumoto, Nakagaki, Nakatani, and Kitagawa (2005)] analyzed the stress distribution in front of the crack tip in an amorphous metal and found that the linear elastic solution agrees with the MD simulation. [ Guo, Wang, Zhao, and Wu (2007)] found that the local stress at the crack tip plays an important role in the mechanism martensitic phase transformation by molecular dynamics simulation of the stress-induced martensitic phase transformation at the crack tip in body-centered cubic structural metals and alloys. [Xu and Deng (2008)] investigated nano-scale void nucleation and growth in a single crystal aluminum and obtained an important finding from MD simulation is that atomic stress plays a controlling role in nano-scale fracture. [Krull and Yuan (2011)] also investigated ductile crack growth in the nano-scale single-crystal aluminum and characterized void nucleation and final crack growth by the stress concentrations at a certain distance from the crack tip. The above studies have shown that consideration of the atomic stress field around the crack tip is important in understanding nano-scale fracture events. Recently, [Wu and Yao (2012)] illuminated the stress distribution around the crack tip is related to the microstructure evolution during the crack propagation by MD simulation. The crack propagation in nickel not only depends on the load but also on the various types of defects present (dislocations, voids, twins) [Karimi, Roarty, and Kaplan (2006)].

From the micro-mechanics viewpoint, the effect of sample size is mainly attributable to the distribution of dislocation density, which induces the change of atomistic

structure around the crack tip during crack propagation. When a pre-cracked crystal deforms plastically in the crack tip region, inhomogeneous dislocations are generated as a diverse form in the crystal [Byon, Kim, and Lee (2007)]. The response of fracture in the crystal metals to the sample size is a complicated phenomenon, involving many physical mechanisms, such as dislocation motions [Yamakov, Wolf, Salazar, Phillpot, and Gleiter (2001); Volkert and Lillodden (2006)], stacking fault energy [Rester, Motz, and Pippin (2008); Yamakov, Wolf, Phillpot, Mukherjee, and Gleiter (2004)], deformation twinning [Wu and Zhu (2008); Yu, Shan, Li, Huang, Xiao, Sun, and Ma (2010)], and phase transformations [Kitakami, Sato, and Shimada (1997)]. These microstructure evolutions of atoms around the crack tip may result in a change of stress field around the crack tip and severely affect the fracture properties of material, such as the twins and dislocation slip, have been considered as a contributing deformation mechanism [Warner, Curtin, and Qu (2007)] and significantly affect the crack propagation [Guo, Wang, and Wang (2004)]. Most experimental evidence have been illustrated a strongly influence of the sample size on the mechanical properties and microstructure evolution of materials at nanometer scale [Uchic, Dimiduk, Florando, and Nix (2004); Greer, Oliver, and Nix (2005); Dimiduk, Uchic, and Parthasarathy (2005); Shan, Mishra, Asif, Warren, and Minor (2008); Lam, Keung, and Tong (2010)]. In order to clarify the sample size induces the change of stress field and crack propagation dynamics in essence, it is essential and important for understanding nano-scale fracture properties by analyzing the atomic stress field and relation to the microstructure evolution around the crack tip. In this paper, MD simulations are performed to investigate the change of sample size induces the microstructure and stress evolutions around the crack tip during crack propagation for a pre-cracked single crystal nickel. The objective of the present work is to determine the relationship between stress distribution around the crack tip and microstructure evolution, and to offer an explanation for the influence of the microstructure evolution caused by the change of sample size on the crack propagation dynamics and stress distribution.

## **2 Modeling and simulation**

### ***2.1 MD simulation and model geometry***

In this work, we perform MD simulations of crack propagation in a pre-cracked single crystal nickel with different sample sizes to investigate the internal microstructural evolution around the crack tip and its influence on the stress field around the crack tip and crack propagation dynamics. MD simulation describes motions of all atoms in a system by numerically solving Newton's equations. The equations

of motion for an atom are given by

$$F_i = m_i \ddot{r}_i \quad (1)$$

where  $m_i$  and  $r_i$  are the mass and position of atom  $i$ , respectively.  $\ddot{r}_i$  is the double time derivative of  $r_i$ , and  $F_i$  is the total interaction force on atom  $i$  by its neighbors. In MD simulations the interaction force  $F_i$  is calculated by the gradient of the total inter-atomic potential  $E$  of the atomic system through

$$F_i = -\nabla_i E(r_1, r_2, \dots, r_n) \quad (2)$$

where  $r_1, r_2, \dots, r_n$  are the positions of the atoms in an atomic system with  $n$  atoms. Once the inter-atomic potential is known for an atomic system under the given initial conditions, an understanding of the material behavior of the system can be achieved through MD simulations. For FCC metallic materials the embedded-atom-Method (EAM) is one of the most popular inter-atomic potentials [Daw, Foiles, and Baskes (1993)]. In the present study the EAM potential provided in [Mishin, Farkas, Mehl, and Papaconstantopoulos (1999)] is used to simulate failure process of a pre-cracked single crystal nickel with unequal sample sizes, considering that this potential has a good ability to describe the bonding in metallic systems and account for dependence of the strength of individual bonds on the local environment, such as surface and defects so that a reasonable simulation of fracture and damage could be obtained [Xu and Deng (2008); Krull and Yuan (2011); Wu and Yao (2012)].

In our MD simulations, a constrained three-dimensional (3D) model is employed for the study of failure in FCC single crystal nickel under mode I loading condition, the geometry of the system of the crack propagation is shown in Fig. 1. The crystal is in the cubic orientation (i.e.  $X$ -[100],  $Y$ -[010], and  $Z$ -[001]). In the model, an edge crack is inserted on the left side of the crystal by removing atoms, the length of the initial crack is equal to  $10a$  ( $35.2 \text{ \AA}$ ) and its width  $a$  ( $3.52 \text{ \AA}$ ), where  $a$  ( $a=3.52 \text{ \AA}$ ) is the lattice constant of nickel. To study the effects of sample size on the stress distribution and microstructure evolution around the crack tip during crack propagation under mode I loading condition, we set up three different blocks of single crystal nickel ( $X \times Y \times Z$ ):  $50a \times 25a \times 6a$  ( $176 \text{ \AA} \times 88 \text{ \AA} \times 21.12 \text{ \AA}$ )  $100a \times 50a \times 6a$  ( $352 \text{ \AA} \times 176 \text{ \AA} \times 21.12 \text{ \AA}$ ), and  $200a \times 100a \times 6a$  ( $704 \text{ \AA} \times 352 \text{ \AA} \times 21.12 \text{ \AA}$ ), the size of crack remain invariable in three models. The crystal dimension in the  $X$ -axis is chosen to be sufficiently long so that steady-state crack propagation is obtained during MD simulations. The right side of the crystal is fixed for motions in  $X$ -direction to limit boundary effects. The atoms in the top and bottom layer, which have a thickness of potential cut-off distance, are fixed. Periodic boundary conditions are formulated in the  $Z$  direction, and non-periodic boundary conditions are

applied in the  $X$  and  $Y$  directions. Because of the use of the periodic condition and a small number of lattice layers in the thickness ( $Z$ ) direction, this 3D model is called a constrained 3D model.

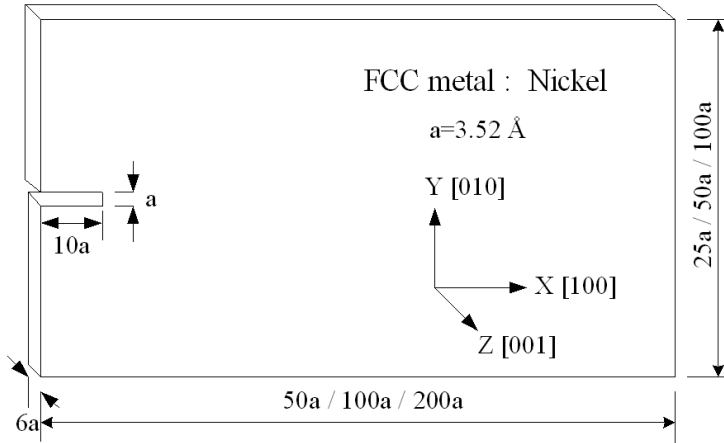


Figure 1: The sample geometry of a FCC single crystal nickel containing a single edge crack.

## 2.2 Simulation process and stress definition

At the start of simulation, this atomic system is relaxed using the conjugate gradient method to reach a minimum energy state. Then the relaxed system is stretched in  $y$ -direction by an incrementally displacement loading every 20ps, by keeping the top and bottom boundary parallel. The global strain rate is  $2.0 \times 10^8 \text{ s}^{-1}$ . Finally the deformed configuration of the system is computed by MD simulation, where the simulation is carried out by integrating Newton's equations of motion for all atoms using a time step of  $1 \times 10^{-15} \text{ s}$ . All simulations are conducted at temperature of  $1 \text{ e-}4 \text{ K}$  (approximately 0 K) using a method to rescale the velocities of the atoms to avoid thermal activation. The open source MD code LAMMPS [Plimpton (1995)] and the visualization tools AtomEye [Li (2003)] are used in the atomistic simulations.

To study the nanoscale fracture behavior and investigate the atomic stress fields around the crack tip during the fracture process, the atomistic stress definition is employed in this work. The atomic stress at an atom is a stress quantity at the atomic scale. Many definitions of atomic stress have been proposed in the past few decades. [Shen and Atluri (2004)] summarized these different definitions of atomic stress and proposed a new atomistic stress formulation with physical clarity, based on the SPH method. In this paper, the atomistic level stress tensor is defined by

strength theory, it is a strength measurement of the inter atomic interactions of the atom with its neighboring atoms, this atomic stress tensor is defined as [Born and Huang (1954)]

$$\sigma_{\alpha\beta}(i) = -\frac{1}{2\Omega_i} \sum_{j \neq (i)}^N f_{\alpha}(i, j) r_{\beta}(i, j) \quad (3)$$

where  $N$  is the number of atoms in a region around atom  $i$  within an EAM potential cut-off distance (which is 4.80 Å for Ni),  $f_{\alpha}(i, j)$  is the vector component form of the interaction force exerted by atom  $j$  on atom  $i$ ,  $r_{\beta}(i, j)$  is the vector component form of the relative position from atom  $j$  to atom  $i$ , and  $\Omega_i$  is the volume of atom  $i$  given by

$$\Omega_i = \frac{4}{3} \pi R_i^3 \quad (4)$$

where  $R_i$  is the radius of the atom  $i$ .

Taking an average over the volume around atom  $i$  within the potential cut-off distance, the average atomic stress tensor  $\bar{\sigma}_{\alpha\beta}(i)$  at atom  $i$  is given by [Horstemeyer and Baskes(1999)]

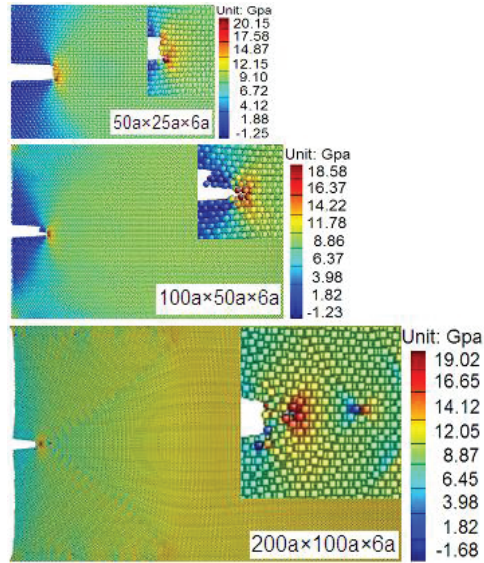
$$\bar{\sigma}_{\alpha\beta}(i) = \frac{1}{N} \sum_{j=1}^N \sigma_{\alpha\beta}(j) \quad (5)$$

### 3 Simulation results

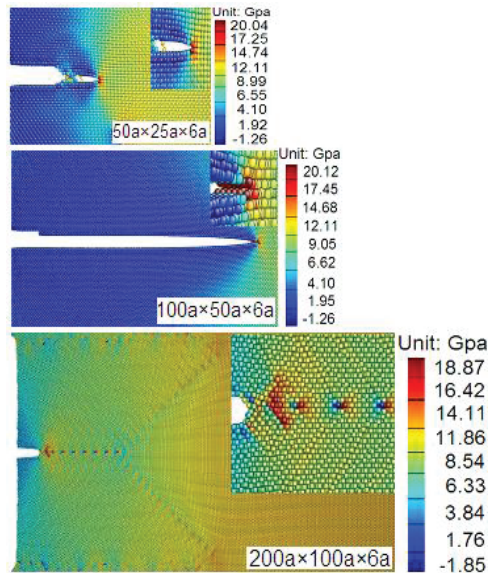
#### 3.1 The crack propagation and stress distribution

Fig.2 shows the crack propagation process and atomic stress distribution around the crack tip of three unequal sample sizes of single crystal nickel at different loading time steps. At the time of  $t=340\text{ps}$ , for a small sample size  $50a \times 25a \times 6a$ , the crack initiation does not occur, the atomic tensile stress is directly concentrated at the crack tip. The crack has initiated and propagated a very short distance along the crack path for a middle sample size  $100a \times 50a \times 6a$ , the stress concentrations also occur at the crack tip of growing crack. However, for a large sample size  $200a \times 100a \times 6a$ , it is found that the crack tip blunting and the concentrations of the atomic tensile stress at a certain distance ahead of the crack tip, as shown in Fig. 2a.

As loading steps increasing at  $t=380\text{ps}$ , the pre-cracked single crystal nickel with three unequal sample sizes show distinctly different of crack propagation states and stress distributions. As seen in Fig. 2b, the void nucleation and growth occurs for a small sample size  $50a \times 25a \times 6a$ , and the peak stress is accompanied by the



(a)  $t=340\text{ps}$



(b)  $t=380\text{ps}$

Figure 2: Contour plots of the atomic tensile stress field for a pre-cracked single crystal nickel with unequal sample sizes at different loading time steps (a)  $t=340\text{ps}$  and (b)  $t=380\text{ps}$ . The insets in the Fig.2 show the atoms and their stress levels around the crack tip.

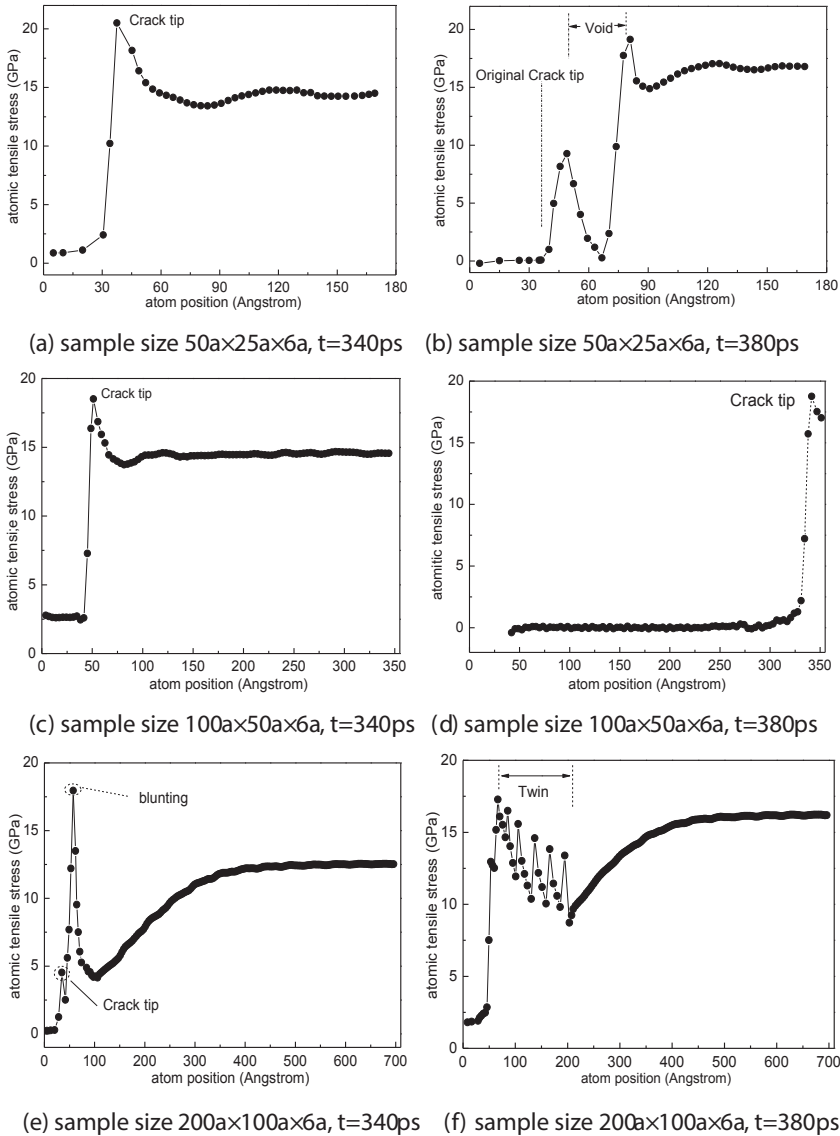


Figure 3: The atomic tensile stress as function of the atom position along the crack path for three unequal sample sizes at t=340ps and t=380ps.



appearance of the void at the location of the atomic tensile stress concentrations. Whereas, for a middle sample size  $100a \times 50a \times 6a$ , the crack straightly extension along the (100) plane and the atomic tensile stress is still concentrated at the crack tip of growing crack. The crack extension represents a brittle character and finally forms a cleavage crack in this case. For a large sample size  $200a \times 100a \times 6a$ , it is more arresting that the crack could hardly propagate and the stress distributions around the crack tip distinctly change, the insets in Fig. 2 provide a detailed view of the atoms and their stress levels around the crack tip.

To provide a more quantitative understanding of stress field around the crack tip for unequal sample sizes at  $t=340\text{ps}$  and  $t=380\text{ps}$ , the atomic tensile stress as function of the atom position along the crack path is plotted in Fig. 3. At  $t=340\text{ps}$ , the crack tip atoms have the highest stress values (approximately 20 GPa and 19 GPa) for sample sizes  $50a \times 25a \times 6a$  and  $100a \times 50a \times 6a$ , respectively, and the stresses are monotonic to the atom position along the crack tip, as shown in Figs. 3a and 3c. For a sample size  $200a \times 100a \times 6a$ , Fig. 3e shows that the stress concentrations occur at a certain distance ahead of the crack tip and the peak stress value is about 19 GPa, but the stress is variable to the atom position along the crack path due to the occurrence of the crack tip blunting.

At the time of  $t=380\text{ps}$ , the atomic tensile stress has a peak value (approximately 19 GPa) at the location of void nucleation for a small sample size  $50a \times 25a \times 6a$  (see Fig. 3b). The stress concentrations and its peak value are still at the crack tip of growing crack for a middle sample size  $100a \times 50a \times 6a$ , as shown in Fig. 3d. However, for a large sample size  $200a \times 100a \times 6a$ , it is a significantly change in the stress distribution around the crack tip along the crack path. It does not show a stress concentration at the crack tip, the high stress values not only occur at the crack tip but also at the plastic region due to the generation of a larger number of deformation twinning ahead of crack tip, as shown in Fig. 3f. It reveals that the plastic deformation around the crack tip induces the change of stress concentrations at the crack tip, and the stress is variable to the atom position along the crack path.

### 3.2 The microstructure evolution around the crack tip

The microstructure evolution around the crack tip in metals is among the most basic problems in mechanics of materials. The plastic processes at the crack tips, including void nucleation and growth [Xu and Deng (2008); Krull and Yuan (2011); Wu and Yao (2012)], dislocation emission [Farkas, Duranduru, Curtin, and Ribbens (2001)], and deformation twinning [Hai and Tadmor (2003)], have a pronounced effect on the stress distributions near the growing crack. This effect is best revealed by a one-to-one relationship between the stress distribution and microstructure characteristic around the crack tip in Fig. 4. For a small sample size  $50a \times 25a \times 6a$ ,

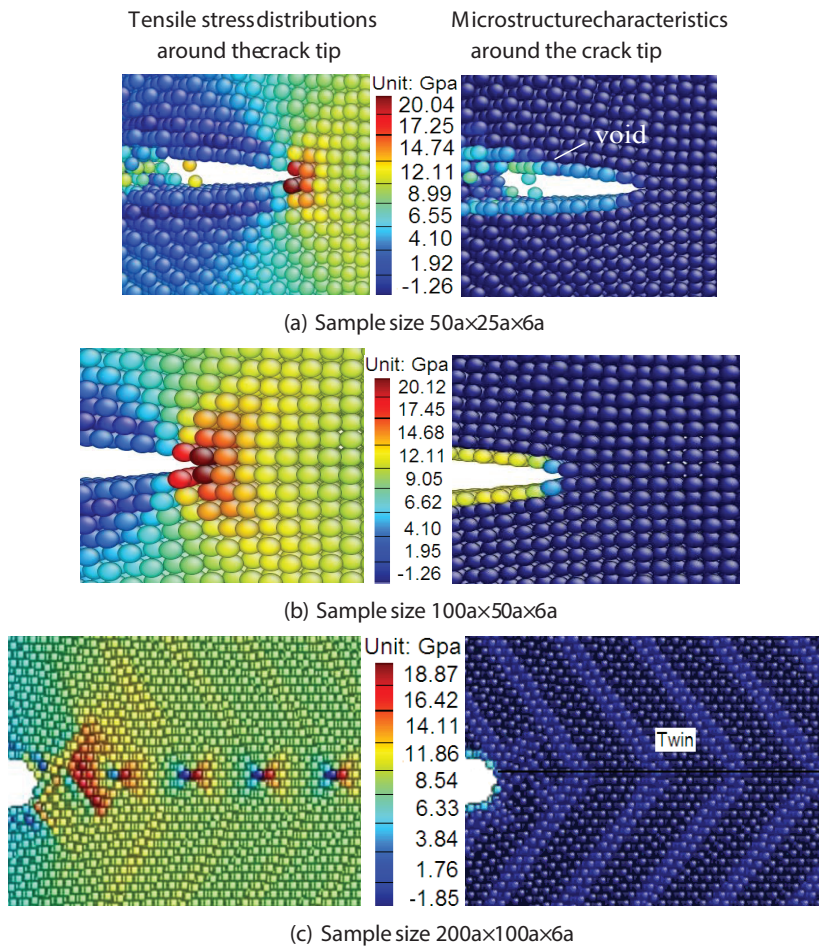


Figure 4: The atomic tensile stress distributions and microstructure characteristics around the crack tip at  $t=380ps$  for unequal sample sizes. (a) sample size  $50a \times 25a \times 6a$ , (b) sample size  $100a \times 50a \times 6a$  and (c) sample size  $200a \times 100a \times 6a$ .

a void is nucleated where the atomic tensile stress has a peak value at a certain distance ahead of the crack tip. The peak stress is accompanied by the appearance of the void at the location of the tensile stress concentrations (see Fig. 4a). For a middle sample size  $100a \times 50a \times 6a$ , the atomic tensile stress concentrates at the crack tip through the fracture process. The analysis of microstructure shows that there is not dislocation emission around the crack tip, as illustrated in Fig. 4b. Therefore, these atoms at the crack tip have the highest stress and energy values, which lead

to the crack growth rapidly along the crack plane. However, for a large sample size  $200a \times 100a \times 6a$ , deformation twinning occurs due to the emissions of partial dislocations from sample boundaries, the stress concentrations does not occur at the crack tip, the atoms of high stress values are not only at the crack tip but also at the region of deformation twinning, especially, at the nodes of deformation twinning, as shown in Figs. 3f and 4c.

### 3.3 crack propagation dynamics and stress-strain curves

Crack propagation dynamics is an important aspect for understanding the crack growth and fracture behavior. In order to show quantitatively the sample size effect on the crack resistance and crack propagation dynamics, the crack propagation length is calculated by the change of the surface energy during the total run time. The crack is expected to propagate along the direction where the newly created surface energy is lowest. The energy of crack growth initiation is defined as the threshold energy and used to determine the crack length. Then the crack length is calculated every 1ps for a total of run time 600ps. The results for the crack length as a function of time for three unequal sample sizes are shown in Fig. 5. It can be seen from Fig. 5 that the crack does not propagates until about 300ps for a middle sample size  $100a \times 50a \times 6a$ , then the crack rapidly propagates and reaches the maximum crack length  $352\text{\AA}$  with increasing the loading time. For a small sample size  $50a \times 25a \times 6a$ , compared with the middle sample size  $100a \times 50a \times 6a$ , the crack extension displays a relatively slow due to the void nucleation during the crack propagation, the crack length does not rapidly increase until about 400ps. Dissimilarly, for a large sample size  $200a \times 100a \times 6a$ , the crack arrests quickly and almost not propagate any further within the calculated loading time steps. Therefore, the crack length almost remains the initial length, even if at the end of run time  $t=600\text{ps}$ , the crack length eventually increases less than  $10\text{\AA}$ . The inset in Fig. 5 provide a more detailed view of the crack extension levels as the loading time increase for a large sample size  $200a \times 100a \times 6a$ .

The size effects on the plasticity of surface-confined single crystals have drawn considerable attention, it has been demonstrated that sample size strongly influences the microstructure and plasticity deformation [Yamakov, Wolf, Salazar, Phillpot, and Gleiter (2001); Horstemeyer, Baskes, and Plimpton (2001)]. To analyze the plastic flow behavior of the growing crack at unequal sample sizes, the stress-strain curves for a pre-cracked single crystal nickel are presented. The averaged atomic stress is used to determine the stress-strain curves for single crystal nickel with unequal sample sizes. Fig. 6 shows the stress-strain curves for a single crystal nickel containing an edge crack at unequal sample sizes. It can be seen from Fig. 6 that there is a stress oscillation for a small sample size  $50a \times 25a \times 6a$  and a stress

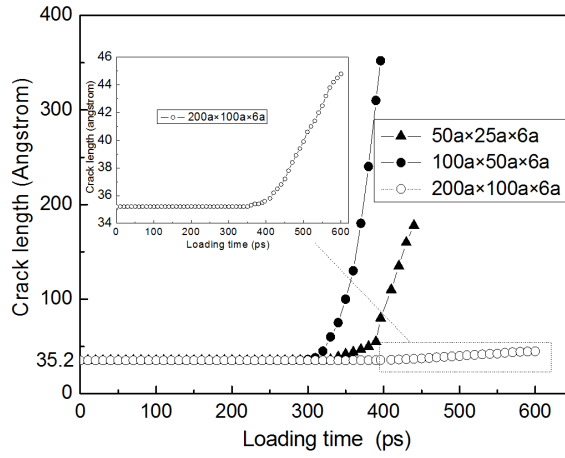


Figure 5: Crack length as a function of loading time for a pre-cracked single crystal nickel with unequal sample sizes.

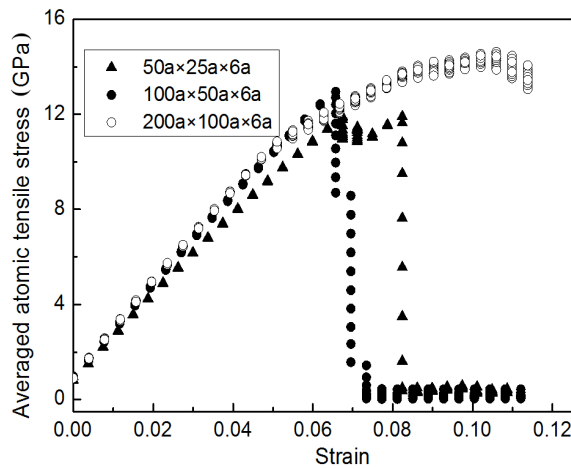


Figure 6: The averaged atomic stress-strain responses for a pre-cracked single crystal nickel with unequal sample sizes.

drop-off rapidly for a middle sample size  $100a \times 50a \times 6a$ . Moreover, the stress oscillations are attenuated as the size increases, these local effects are weakened by size increasing due to a global stress averaging procedure [Horstemeyer, Baskes, and Plimpton (2001)]. Compared with three unequal sample sizes, a remarkable difference in plastic flow behavior for a large sample size  $200a \times 100a \times 6a$ , there are not oscillations and stress drop-offs but a strain-hardening occurs in the stress-strain curves as shown in Fig. 6. This comparison of stress-strain curves for unequal sample sizes illustrating different plasticity regions, there is a gradual change of influence from the void nucleation and growth at a small sample size to the formation of deformation twinning around the crack tip at a large sample size. It reveals that the change of sample size induces the microstructure evolution around the crack tip determining the stress states and plastic deformation. The above results further emphasize that the microstructure evolution, especially the formation of deformation twinning around the crack tip affect the crack propagation dynamics and plastic flow behavior, which are associated with a distinct change in the atomistic deformation mechanism.

#### **4 Discussion and Conclusions**

At low temperature, the two major mechanisms responsible for the plasticity of materials are ordinary dislocation plasticity and deformation twinning [Yamakov, Wolf, Phillpot, and Gleiter (2002); Reed (1967); Haasen (1958)]. Crack-tip microstructures, including deformation twinning and dislocation emission, have a pronounced effect on the stress distribution around the crack tip of growing crack. The sample size effect is mainly attributable to the distributions of dislocation density, inhomogeneous dislocations are generated as a diverse form in the crystal under the loading, which induces the atomistic structure and stress field change around the crack tip during crack propagation. For a small sample size  $50a \times 25a \times 6a$ , void nucleation occurs at a certain distance ahead of the crack tip where the atomic tensile stress concentrations, and the peak stress is accompanied by the appearance of the void at the location of the stress concentrations. The stress is variable to the atom position along the crack path due to the peak stress occurs at the location of the void nucleation. For a middle sample size  $100a \times 50a \times 6a$ , there are almost not dislocation emissions at the crack tip. The atomic tensile stress is always concentrated at the crack tip of growing crack, so the stress is monotonic to the atom position along the crack path. When the sample size is increased, for a large sample size  $200a \times 100a \times 6a$ , deformation twinning occurs due to the emissions of partial dislocations from sample boundaries, it does not show stress concentrations at the crack tip, the high stress values occur not only at the crack tip atoms but also at deformation twinning atoms. Accordingly, the stress is variable to the atom position along

the crack path due to the formation of deformation twinning induces the change of stress distribution.

In addition, the current simulations are performed under a special atomistic configuration, it is noteworthy that boundary effect could not be ignored due to the restriction of model and boundary conditions. When the initial crack length remains constant in the samples, the boundary effects become more prominent with the increase of sample size. In contrary, the smaller of sample size is, the more prominent of the effect of initial defect (crack) is. In view of this, for a large sample size  $200a \times 100a \times 6a$ , it is easily favorable to generate partial dislocations from sample boundaries at the applied loading. The dislocations are continually emitted from two boundaries (up and down) as the application of loading, finally form deformation twinning along the direction of crack propagation ahead of the crack tip. It is well known that dislocation emission and twinning are important complementary mechanisms for plastic deformation in many metallic systems, and twinning has been identified as a contributing plastic deformation mechanism in nanocrystalline metals [Warner, Curtin, and Qu (2007); Reed (1967); Haasen (1958); Feng, Cheng, Wu, Wang and Hong (2006)]. Due to a large number of deformation twins occur ahead of the crack tip, which can effectively relax the local stress at the crack tip and act as a barrier to further crack propagation, therefore, the crack is difficult to further propagate in this case. It indicate that the void nucleation, especially deformation twinning formation around the crack tip severely affect the crack propagation and stress distribution, the crack propagation and resistance behavior are much related to the internal microstructure evolution around the crack tip.

As discussed above, it can be concluded that the crack propagation dynamics and stress distributions around the crack tip are strongly dependent on the change of sample size induces the microstructure evolution during growing crack. If the atomic configuration does not change around the crack tip, the crack propagates rapidly along the crack path, the stress is always concentrated at the crack tip of growing crack and the stress is monotonic to the atom position along the crack path. Once the atomic configuration around the crack tip is changed, such as void nucleation and deformation twinning, the crack growth becomes slow and induces the change of stress distributions around the crack tip. Simultaneously, the stress is variable to the atom position along the crack path. In a word, the single crystal nickel with a surface crack under a constant mode I loading condition shows the different crack propagation dynamics and stress distributions, which are directly linked to the sample size induces the void nucleation and deformation twinning mechanisms around the crack tip.

## Acknowledgements

The work was supported by National Natural Science Foundation of China (Grant No. 11102139), and China Postdoctoral Science Foundation (Grant Nos. 20110491205 and 2012T50665).

## References

**Born, M.; Huang, K.** (1954): *Dynamical theory of crystal lattices*. Oxford, Clarendon.

**Buehler, M. J.; Gao, H. J.; Huang, Y. G.** (2004): Atomistic and continuum studies of stress and strain fields near a rapidly propagating crack in a harmonic lattice. *Theor. Appl. Fract. Mech.*, vol.41, no.1-3, pp.21-42.

**Byon, S. M.; Kim, H. S.; Lee, Y.** (2007): Investigation of the size effect on the crack propagation using finite element method and strain gradient plasticity. *J. Mater. Process Technol.*, vol.191, no.1-3, pp.193-197.

**Cheung, K. S.; Yip, S.** (1994): A molecular-dynamics simulation of crack-tip extension: the brittle-to ductile transition. *Modelling Simul. Mater. Sci. Eng.*, vol. 2, no.4, pp. 865-892.

**Daw, M. S.; Foiles, S. M.; Baskes, M. I.** (1993): The embedded-atom method: a review of theory and applications. *Mater. Sci. Rep.*, vol. 9, no.7-8, pp.251-310.

**Dimiduk, D. M.; Uchic, M. D.; Parthasarathy, T. A.** (2005): Size-affected single-slip behavior of pure nickel microcrystals. *Acta Mater.*, vol.53, no.15, pp.4065–4077.

**Farkas, D.; Duranduru, M.; Curtin, W. A.; Ribbens, C.** (2001): Multiple-dislocation emission from the crack tip in the ductile fracture of Al. *Philos. Mag. A*, vol. 81, no.5, pp.1241-1255.

**Feng, X. Y.; Cheng, Z. Y.; Wu, X.; Wang, T. C.; Hong, Y. S.** (2006): Twinning in nanocrystalline Ni by severe plastic deformation. *J. Phys. D: Appl. Phys.*, vol. 39, no.4, pp.746-749.

**Greer, J. R.; Oliver, W. C.; Nix, W. D.** (2005): Size dependence of mechanical properties of gold at the micro scale in the absence of strain gradients. *Acta Mater.*, vol.53, no.6, pp.1821-1830.

**Guo, Y. F.; Wang, C. Y.; Wang, Y. S.** (2004): The effect of stacking fault or twin formation on bcc-iron crack propagation. *Phil. Mag. Lett.*, vol. 84, no.12, pp.763-770.

**Guo, Y. F.; Wang, Y. S.; Zhao, D. L.; Wu, W. P.** (2007): Mechanisms of martensitic phase transformations in body-centered cubic structural metals and alloys:

Molecular dynamics simulations. *Acta Mater.*, vol. 55, no.19, pp.6634-6641.

**Haasen, P.** (1958): Plastic deformation of nickel single crystals at low temperatures. *Philos. Mag.*, Vol. 3, no.28, pp. 384-418.

**Hai, S.; Tadmor, E. B.** (2003): Deformation twinning at aluminum crack tips. *Acta Mater.*, vol.51, no.1, pp.117-131.

**Horstemeyer, M. F.; Baskes, M. I.** (1999): Atomistic finite deformation simulations: a discussion on length scale effects in relation to mechanical stresses. *ASME-Trans: J. Eng. Mater. Technol.*, Vol: 121, no.2, pp. 114-119.

**Horstemeyer, M. F.; Baskes, M. I.; Plimpton, S. J.** (2001): Length scale and time scale effects on the plastic flow of FCC Metals. *Acta Mater.*, vol. 49, no.20, pp.4363-4374.

**Karimi, M.; Roarty, T.; Kaplan, T.** (2006): Molecular dynamics simulations of crack propagation in Ni with defects. *Modelling Simul. Mater. Sci. Eng.*, vol.14, no.8, pp.1409-1420.

**Kitakami, O.; Sato, H.; Shimada, Y.** (1997): Size effect on the crystal phase of cobalt fine particles. *Phys. Rev. B*, Vol.56, no.21, pp.13849-13854.

**Krull, H.; Yuan, H.** (2011): Suggestions to the cohesive traction-separation law from atomistic simulations. *Eng. Fract. Mech.*, vol.78, no.3, pp.525-533.

**Lam, D. C. C.; Keung, L. H.; Tong, P.** (2010): Size-Dependent Behavior of Macromolecular solids II: Higher-Order Viscoelastic Theory and Experiments. *CMES: Computer Modeling in Engineering & Sciences*, Vol. 66, no.1, pp.73-99.

**Li, J.** (2003): Atomeye: an efficient atomistic configuration viewer. *Model. Simul. Mater. Sci. Eng.*, vol.11, no.2, pp.173-177.

**Matsumoto, R.; Nakagaki, M.; Nakatani, A; Kitagawa, H.** (2005): Molecular-dynamics study on crack growth behavior relevant to crystal nucleation in amorphous metal. *CMES: Computer Modeling in Engineering & Sciences*, vol. 9, no.1, pp.75-84.

**Mishin, Y.; Farkas, D.; Mehl, M. J.; Papaconstantopoulos, D. A.** (1999): Interatomic potentials for monoatomic metals from experimental data and ab initio calculations. *Phys. Rev. B*, vol.59, no. 5, pp.3393 -3407.

**Nishimura, K.; Miyazaki N.** (2001): Molecular dynamics simulation of crack propagation in polycrystalline material. *CMES: Computer Modeling in Engineering & Sciences*, vol. 2, no. 2, pp.143-154.

**Plimpton, S. J.** (1995): Fast parallel algorithms for short-range molecular dynamics. *J. Comput. Phys.*, vol. 117, pp.1-19. <http://lammps.sandia.gov/>.

**Reed, R.P.** (1967): Deformation twinning in Ni and F.C.C Fe-Ni alloys. *Philos.*



*Mag.*, vol. 15, no.137, pp. 1051-1055.

**Rester, M.; Motz, C.; Pippin, R.** (2008): Stacking fault energy and indentation size effect: Do they interact ? *Scripta Mater.*, vol.58, no.3, pp.187-190.

**Shan, Z. W.; Mishra, R. K.; Asif, S. A. S.; Warren, O. L.; Minor, A. M.** (2008): Mechanical annealing and source-limited deformation in submicrometre-diameter Ni crystals. *Nature Mater.*, vol.7, pp.115-119.

**Shen, S.; Atluri, S. N.** (2004): Atomic-level stress calculation and continuum molecular system equivalence. *CMES: Computer Modeling in Engineering & Sciences*, vol. 6, no.1, pp.91-104.

**Uchic, M. D.; Dimiduk, D. M.; Florando, J. N.; Nix, W. D.** (2004): Sample dimensions influence strength and crystal plasticity. *Science*, vol. 35, no.5686, pp.986-989.

**Volkert, C. A.; Lillodden, E. T.** (2006): Size effects in the deformation of sub-micro Au columns. *Philos. Mag.*, vol.86, no. 33-35, pp.5567-5579.

**Warner, D. H.; Curtin, W. A.; Qu, S.** (2007): Rate dependence of crack-tip processes predicts twinning trends in f.c.c. metals. *Nature Mater.*, vol. 6, no.12, pp.876-881.

**Wu, X. L.; Zhu, Y. T.** (2008): Inverse grain-size effect on twinning in nanocrystalline Ni. *Phys. Rev. Lett.*, vol.101, no.2, pp.025503.

**Wu, W. P.; Yao, Z. Z.** (2012): Molecular dynamics simulation of crack tip stress and microstructure evolution of a growing crack in single crystal nickel. *Thero. Appl. Fract. Mech.*, Vol. 62, pp. 67-75.

**Xu, S.; Deng, X.** (2008): Nanoscale void nucleation and growth and crack tip stress evolution ahead of a growing crack in a single crystal. *Nanotechnology*, vol.19, no.11, pp.115705.

**Yamakov, V.; Wolf, D.; Salazar, M.; Phillpot, S. R.; Gleiter, H.** (2001): Length-scale effects in the nucleation of extended dislocations in nanocrystalline Al by molecular dynamics simulation. *Acta Mater.*, vol.49, no.14, pp.2713-2722.

**Yamakov, V.; Wolf, D.; Phillpot, S. R.; Gleiter, H.** (2002): Deformation twinning in nanocrystalline Al by molecular dynamics simulation. *Acta Mater.*, vol.50, no.20, pp.5005-5020.

**Yamakov, V.; Wolf, D.; Phillpot, S. R.; Mukherjee, A. K.; Gleiter, H.** (2004): Deformation-mechanism map for nanocrystalline metals by molecular-dynamics simulation. *Nature Mater.*, vol. 3, no.1, pp. 43-47.

**Yamakov, V.; Saether, E.; Phillips, D. R.; Glaessgen, E.H.** (2006): Molecular-dynamics simulation-based cohesive zone representation of intergranular fracture processes in aluminum. *J. Mech. Phys. Solids*, vol. 54, no.9, pp.1899-1928.

**Yu, Q.; Shan, Z. W.; Li, J.; Huang, X.; Xiao, L.; Sun, J.; Ma, E.** (2010): Strong crystal size effect on deformation twinning. *Nature*, vol.463, pp.335-338.

**Zhou, X. W.; Zimmerman, J.A.; Reedy Jr., E.D.; Moody, N. R.** (2008): Molecular dynamics simulation based cohesive surface representation of mixed mode fracture. *Mech. Mater.*, vol. 40, no.10, pp. 832-845.